Pigford, R. L. and G. Sliger, "Rate of Diffusion Controlled Reaction Between a Gas and a Porous Solid Sphere," *Ind. Eng. Chem. Process Design Develop.*, **12** (1), 85 (1973).
Potter, A. E., "Sulfur Oxide Capacity of Limestones," *Ceramic Bulletin*, **48** (9), 855 (1969).
Ramachandran, P. A. and J. M. Smith, "A Single-Pore Model for Gas-Solid Noncatalytic Reactions," *AIChE J.*, **23** (3), 353 (1977).
Ulerich, N. H., E. P. O'Neill and D. L. Keairns, "The Influence of Limestone Calcination on the Utilization of the Sulfur-Sorbent in Atmospheric Pressure Fluid-Bed Combustors," Westinghouse Electric Report for Electric Power Research Institute (1977).
Vogel, G. J., et al., "Supportive Studies in Fluidized-Bed Combustion," Argonne National Laboratory Report for U.S. Energy Research and Development Administration and U.S. Environmental Protection Agency, ANL/ES-CEN-1019 and FE-1780-7 (April, 1977).
Vogel, G. J., et al., "A Development Program on Pressurized Fluidized-Bed Combustion," Argonne National Laboratory Report for U.S. Energy Research and Development Administration and U.S. Environmental Protection Agency, ANL/ES-CEN-1011 (1975).
Yagi, S. and D. Kunii, "Fluidized-Solids Reactors with Continuous Solids Feed," *Chem. Eng. Sci.*, **16**, 364, 372, 280 (1961).
Yang, R. T., P. T. Cunningham, W. I. Wilson, and S. A. Johnson, "Kinetics of the Reaction of Half-Calcined Dolomite with Sulfur Dioxide," *Adv. in Chem. Ser.*, **139**, 149 (1975).

Manuscript received March 2, 1980; revision received August 8, and accepted August 28, 1980.

Steady-State Uniqueness and Multiplicity of Nonadiabatic Gas-Liquid CSTRs

Part I: Second-Order Reaction Model

D. T.-J. HUANG
and
ARVIND VARMA
Department of Chemical Engineering
University of Notre Dame
Notre Dame, IN 46556

Steady-state behavior of a non-adiabatic gas-liquid CSTR is classified applying a second-order reaction model without any limitation on the reaction regime. Uniqueness and multiplicity regions are determined in the parameter space of reactivity versus liquid residence time, with the ignition and extinction points explicitly shown. An isola with five steady states is found possible for the adiabatic reactor; however, even a small heat loss reduces the number of steady states to three.

SCOPE

In the operation of gas-liquid CSTRs (continuous stirred-tank reactors), the occurrence of multiple steady states has been observed by Ding et al. (1974) for the chlorination of *n*-decane. Hoffman et al. (1975) explored the parametric sensitivity of steady state multiplicity for a second-order reaction in an adiabatic gas-liquid CSTR. Sharma et al. (1976) further carried out numerical simulations of the experimental results of Ding et al. (1974) and showed the possible existence of up to seven steady states for consecutive second-order reactions in a nonadiabatic gas-liquid CSTR. It is thus realized that information regarding parametric sensitivity and behavioral features, particularly the multiplicity patterns and the maximal number of steady state solutions, is essential for the rational design, operation and control of gas-liquid reactors. This raises the need for classifying the steady state behavior in terms of the multiplicity patterns and the ignition and extinction points in different parameter spaces.

The experimental and numerical observations of multiple steady states in gas-liquid CSTRs have prompted development of *a priori* criteria providing conditions among physico-chemical parameters which guarantee unique and multiple steady states. Raghuram and Shah (1977) have derived conditions assuring uniqueness of the steady state and have presented various plots to determine the number of steady states in parameter spaces for the case of pseudo-first-order reactions (i.e., the conversion of the liquid reactant is assumed zero) and for second-order reactions in the "fast" reaction regime, respectively, occurring in an *adiabatic* gas-liquid CSTR. Huang and Varma (1981) provide analytic necessary and sufficient conditions for uniqueness and multiplicity and the stability of the steady state for the case of pseudo-first-order reactions in the "fast" reaction regime, occurring in a non-adiabatic CSTR. However, when multiple steady states exist, the steady state on the high temperature branch is generally in the "fast" reaction regime, and the conversion of the liquid reactant is significant. On the other hand, the steady state on the low temperature branch is usually in the "slow" reaction regime. It is noted that the initial conditions determine the nature of the steady state attained, and ignition or extinction may occur as the physico-chemical parameters are varied. Therefore, these previously reported reaction models with their simplifying assumptions may lead to pitfalls and so should be discriminated.

Previous results as reported by Hoffman et al. (1975) and Sharma et al. (1976) suggest that steady state multiplicity can serve as an excellent tool for discriminating among rival models and assumptions, and for the estimation of kinetic parameters. The main goal of this work is to clarify the steady state behavior in terms of the multiplicity patterns, and the ignition and extinction points, by applying a fully second-order reaction model. In Part II, the results of this work will be used to discriminate among the various reaction models with their simplifying assumptions as described above.

Correspondence concerning this paper should be addressed to A. Varma.
D. T.-J. Huang is presently at Brookhaven National Laboratory, Upton, New York 11973.

CONCLUSIONS AND SIGNIFICANCE

A model is developed for a second-order gas-liquid reaction in a nonadiabatic CSTR without any limitation on the reaction regime. *A priori* bounds are obtained to help in the determination of the steady state solutions. Numerical simulation is carried out to compare the predictions of the model with the experimental results of Ding et al. (1974); the agreement is shown to be good and suggests some capability of the model to describe real systems.

For an adiabatic case, the possible existence of an *isola* with five steady states is shown. However, it is found that a small heat loss by heat transfer through the reactor wall or cooling device can eliminate the possibility of the existence of five steady states. Note that the occurrence of an isola in the *adiabatic* case is a special characteristic of multiphase CSTRs, not found in single-phase reactors.

Steady-state behavior is classified by means of the multiplicity patterns and the ignition and extinction points in the parameter space of reactivity versus liquid residence time. The effect of the activation energy is shown in this parameter space, and it is found that as the activation energy decreases, the multiplicity region shrinks with respect to both the reactivity and liquid residence time. This feature is believed powerful enough to discriminate among rival models and will be applied in Part II. It is also shown that as the heat of reaction increases, the minimal required liquid flow rate to assure uniqueness increases.

Hoffman et al. (1975) suggested that the interactions among the rate of the chemical reaction, the transport resistances, and the solubility cause the occurrence of multiple steady states in gas-liquid reactors. We present various plots showing the features of the reaction factor, the rate of gas absorption, and the concentration of the gaseous reactant in the bulk liquid accompanied with different multiplicity patterns; their relations with one another and with the steady state temperature and the conversion of the liquid reactant are thus clarified. The picture of the reaction factor (or equivalent enhancement factor) corresponding to steady state multiplicity is plotted here, we believe, for the first time; this provides a deeper understanding of the reaction behavior. In addition, it is shown that the limitation the liquid reactant imposes plays an important role in the determination of multiple steady states and should not be overlooked.

ANALYSIS

Second-order kinetics represent the rate of many gas-liquid reactions, such as oxidation, hydrogenation, and chlorination of hydrocarbons and are considered in this work:

$$A\ (\text{gas}) + B\ (\text{liq}) \xrightarrow{k} \text{Products (liq)}$$

The following assumptions are made:

1. The liquid phase consists of nonvolatile components and no evaporation into the gas phase takes place.
2. The physical and thermal properties of the gas and liquid, the interfacial area and gas holdup, the liquid mass transfer coefficient, the diffusion coefficients and the volumetric flow rates of the gas and liquid are independent of temperature and conversion.
3. The solubility of gaseous reactant A follows Henry's law, i.e.

$$A_i = H_o A_g \exp\left[\frac{-\Delta H_s}{RT}\right] \tag{1}$$

where H_o is the Henry's law constant and independent of temperature and conversion.

4. The gas and liquid are at the same temperature within the reactor, and the feed temperatures are the same.
5. The gas phase resistance to mass transfer is negligible.
6. The liquid feed contains no dissolved gaseous reactant.

The steady-state material and energy balances are thus:

$$F_g(A_{gf} - A_g) = R_A V_R + F_l A_l \tag{2}$$

$$F_l(B_{lf} - B_l) = R_A V_R \tag{3}$$

$$(F_g\rho_g C_{Pg} + F_l\rho_l C_{Pl})(T_f - T) + (-\Delta H_s - \Delta H_R)R_A V_R + (-\Delta H_s)F_l A_l - US(T - T_c) = 0 \tag{4}$$

The rate of gas absorption can be expressed as:

$$k_l a A_i V_R E_A^* = R_A V_R + F_l A_l \tag{5}$$

where E_A^* is the reaction factor.

As described by Hoffman et al. (1975), E_A^* and A_l can be computed from the following expressions, which are from the approximate film theory solutions:

$$E_A^* = M\sqrt{b_i}\,\frac{M^2(\alpha' - 1) + \frac{1}{\theta'} + M\sqrt{b_i}\tanh(M\sqrt{b_i})}{\left[M^2(\alpha' - 1) + \frac{1}{\theta'}\right]\tanh(M\sqrt{b_i}) + M\sqrt{b_i}} \tag{6}$$

$$A_l = A_i\,\frac{M\sqrt{b_i}}{M\sqrt{b_i}\cosh(M\sqrt{b_i}) + \left[M^2(\alpha' - 1) + \frac{1}{\theta'}\right]\sinh(M\sqrt{b_i})} \tag{7}$$

where b_i is obtained from:

$$b_i = \frac{E_i - E_A^* - \frac{A_l}{A_i}}{E_i - 1} \tag{8}$$

with

$$E_i = 1 + \frac{D_B B_l}{D_A A_i} \tag{9}$$

$$M = \frac{\sqrt{kD_A B_l}}{k_l} \tag{10}$$

and

$$\alpha' = \frac{\epsilon_l k_l}{a D_A}, \quad \theta' = \frac{k_l a \tau_l}{\epsilon_l} \tag{11}$$

With Eqs. 6 and 7 substituting into Eq. 8, a transcendental expression for b_i is obtained and b_i can then be solved by trial-and-error. Note that Arrhenius equation shows:

$$k = k_o \exp\left(-\frac{E}{RT}\right) \tag{12}$$

The following dimensionless variables are defined:

$$x_g = \frac{A_{gf} - A_g}{A_{gf}} \qquad y = \frac{T - T_f}{T_f}$$

$$\gamma = \frac{E}{RT_f} \qquad y_c = \frac{T_c - T_f}{T_f}$$

$$\delta = \frac{(-\Delta H_s)}{RT_f} \qquad D_g = \frac{k_l a V_R H_o}{F_g}$$

$$\alpha = \frac{F_g\rho_g C_{Pg} + F_l\rho_l C_{Pl}}{F_g\rho_l C_{Pl}} \qquad \beta = \frac{US}{F_g\rho_l C_{Pl}} \qquad (13)$$

$$B = \frac{(-\Delta H_s - \Delta H_R)A_{gf}}{\rho_l C_{Pl} T_f} \qquad p = \frac{(-\Delta H_R)F_l A_{gf}}{F_g\rho_l C_{Pl} T_f}$$

$$Q = \frac{F_g}{F_l} \qquad q = \frac{B_{lf}}{A_{gf}}$$

$$a_l = \frac{A_l}{B_{lf}} \qquad b_l = \frac{B_l}{B_{lf}}$$

Combining Eqs. 2 and 5 leads to, in dimensionless form:

$$x_g - D_g E_A^*(1 - x_g) \exp\left(\frac{\delta}{1 + y}\right) = 0 \qquad (14)$$

from Eqs. 2 and 3, we obtain:

$$b_l = 1 + a_l - \frac{Qx_g}{q} \qquad (15)$$

and combination of Eqs. 4 and 5 leads to:

$$-\alpha y + BD_g E_A^*(1 - x_g) \exp\left(\frac{\delta}{1 + y}\right) - pqa_l - \beta(y - y_c) = 0 \qquad (16)$$

We note that combining Eqs. 14 and 16 gives:

$$-\alpha y + Bx_g - pqa_l - \beta(y - y_c) = 0 \qquad (17)$$

From Eq. 17, we get

$$y = \frac{Bx_g + \beta y_c - pqa_l}{\alpha + \beta} \qquad (18)$$

or

$$x_g = \frac{(\alpha + \beta)y + pqa_l - \beta y_c}{B} \qquad (19)$$

With Eq. 19 substituting into Eq. 16, we obtain a single equation for the dimensionless steady state temperature:

$$-\alpha y + D_g E_A^*[B - (\alpha + \beta)y - pqa_l + \beta y_c] \exp\left(\frac{\delta}{1 + y}\right) - pqa_l - \beta(y - y_c) = 0 \qquad (20)$$

Also, Eq. 1 becomes:

$$A_i = A_{gf} H_o (1 - x_g) \exp\left(\frac{\delta}{1 + y}\right) \qquad (21)$$

and Eq. 12 becomes:

$$k = k_o \exp\left(-\frac{\gamma}{1 + y}\right) \qquad (22)$$

A priori bounds

From physical considerations, we see that the upper temperature bound is with $x_g = 1$ and $a_l = 0$; i.e., all of the gaseous reactant A dissolves into the liquid phase and is completely consumed by reacting with the liquid reactant B there. Note that under certain circumstances, there may not be enough B for this total consumption of A. Similarly, the lower temperature bound is with $x_g = 0$ and $a_l = 0$; i.e., no gaseous reactant enters the liquid phase and thus no reaction occurs at all. It can then be easily shown from Eq. 18 that the dimensionless steady state temperature is bounded in the range:

$$y_{lb} \equiv \frac{\beta y_c}{\alpha + \beta} \le y \le \frac{B + \beta y_c}{\alpha + \beta} \equiv y_{ub} \qquad (23)$$

On the other hand, the conversion of the liquid reactant B, i.e., $x_l = 1 - b_l$, should be bounded by:

$$0 \le x_l \le 1 \qquad (24)$$

It is clear that at $y = y_{lb}$ (i.e., no reaction occurring) $x_l = 0$, and when y increases x_l increases. However, even if $y < y_{ub}$, no further increase of the steady state temperature is possible if all of the liquid reactant has been exhausted. Thus, the conditions $y \le y_{ub}$ and $x_l \le 1$ should be checked *simultaneously*.

From this observation, we see that the numerical trial-and-error procedure of finding the steady state temperature is better started from $y = y_{lb}$.

Numerical Procedure

For a set of physico-chemical parameters and at a prescribed value of y, k is computed from (22). Starting from $y = y_{lb}$ with a suitable step size in y, the corresponding value of a_l at $y = y_{lb}$ is assumed and x_g is computed from Eq. 19. Then, A_i and B_l are obtained through Eqs. 21 and 15, respectively. E_i is then computed from Eq. 9 and M from Eq. 10.

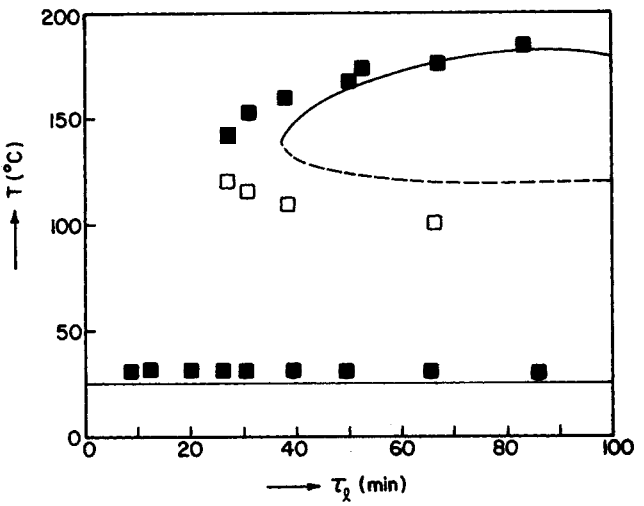

Figure 1. Comparison of predictions of the model with experimental results.

TABLE 1. PARAMETERS USED IN THE SIMULATION OF THE EXPERIMENTAL RESULTS AND IN THE CLASSIFICATION OF STEADY STATE BEHAVIOR.

a	$= 3\ \text{cm}^{-1}$	E	$= 29000$ cal/gmol
$D_A = D_B$	$= 6 \times 10^{-5}\ \text{cm}^2/\text{s}$	$(-\Delta H_R)$	$= 26000$ cal/gmol
k_l	$= 0.04$ cm/s	$(-\Delta H_s)$	$= 4500$ cal/gmol
ρ_{gf}	$= 4.2 \times 10^{-5}$ gmol/cm^3	V_R	$= 400$ cm^3
ρ_{lf}	$= 5.1 \times 10^{-3}$ gmol/cm^3	ϵ_l	$= 0.86$
C_{Pg}	$= 6.5$ cal/gmol · °K	F_g	$= 18.5$ cm^3/s
C_{Pl}	$= 70$ cal/gmol · °K	T_f	$= 297$°K
H_o	$= 0.00188$	T_c	$= 298$°K
A_{gf}	$= 4.2 \times 10^{-5}$ gmol/cm^3	US	$= 0.03$ cal/°K · s
B_{lf}	$= 5.1 \times 10^{-3}$ gmol/cm^3	k (at 50°C)	$= 0.005$ cm^3/gmol · s

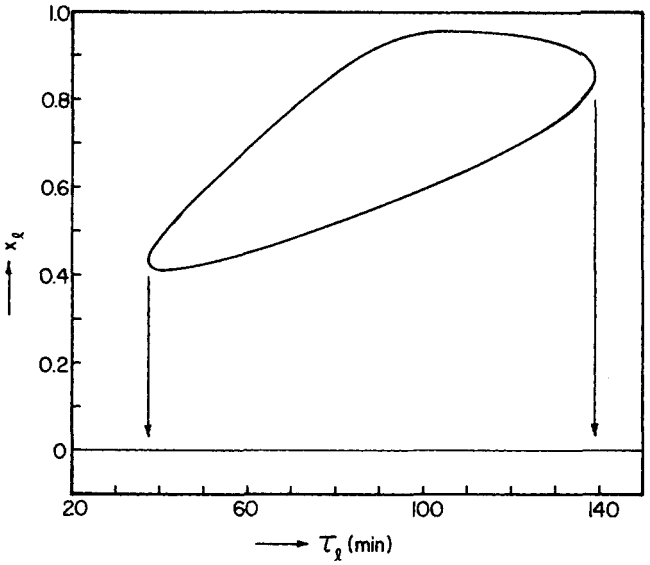

Figure 2a. Effect of liquid residence time on the conversion of liquid reactant.

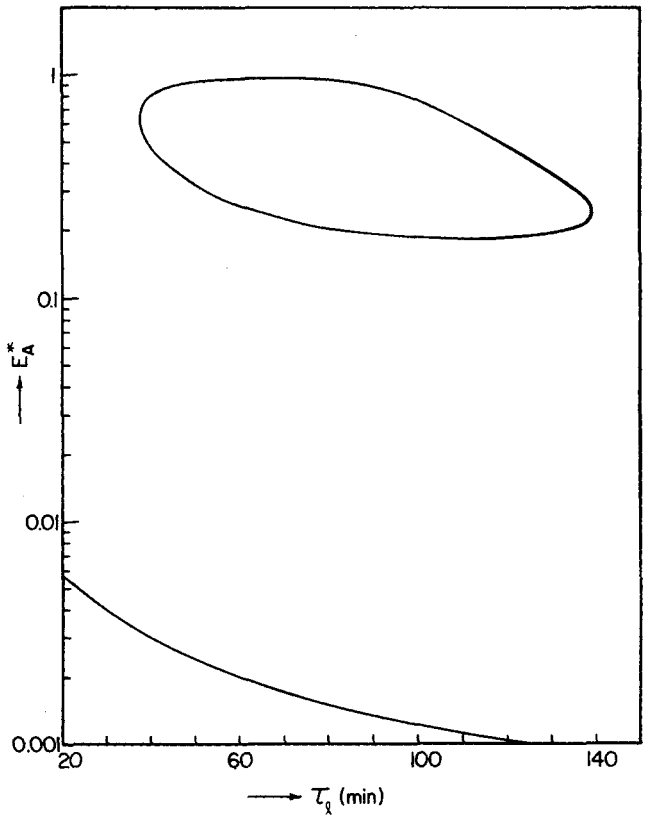

Figure 2b. Effect of liquid residence time on the reaction factor.

With all these values, b_i is solved from Eq. 8 as noted before and E_A^* is then computed from Eq. 6 and a_l from Eq. 7. If this computed value of a_l does not agree with the assumed value, it is set to be the new assumed value and the procedure is repeated. The convergence is found to be rather rapid for all the numerical examples present in this work.

After the convergence of a_l is achieved, the computed values of E_A^* and a_l are substituted into Eq. 20 to check whether this prescribed value of y is a solution or not. For the next value of y, the last converged value of a_l is set as the starting assumed value and one proceeds as before. A half-interval method is used within a stepsize, where a solution is detected, to exactly locate the solution of the steady state temperature.

In this work, the first assumed value of a_l was usually set as 0.01 and it was found that any reasonable a_l value leads to rather fast convergence. Apparently for the above procedure, the assumed value affects only the first step. It should be mentioned here that for very small liquid residence time ($\tau_l \to 0$), i.e., very large liquid flow rate, the temperature is virtually the same as the feed temperature and the liquid bulk concentration of the gaseous reactant A_l is virtually zero, i.e., $a_l = 0$.

We note that in the work of Hoffman et al. (1975), two variables were assumed. In the same manner as described in this work, only the variable A_l needs to be assumed in that work as well; this results in significant savings in computational effort.

NUMERICAL RESULTS AND DISCUSSION

Throughout this work, we consider the case of fixed gas feed rate, i.e., F_g fixed. To test the capability of the model to describe real systems, numerical simulation was carried out to compare its predictions with experimental results on the chlorination of n-decane, reported by Ding et al. (1974) and as presented by Sharma et al. (1976) in their Figure 1. The results are shown in Figure 1 with all the physico-chemical parameters presented in Table 1, as reported by Sharma et al. (1976) in their Table 1 and with some physical properties reported by Hoffman et al. (1975) for the same experiments. It is seen that the agreement is quite good and thus may suggest the applicability of the model to that experimental system.

From Figures 2a, b and also 3, an *isola* is predicted for this case, where as the liquid residence time τ_l increases beyond the experimental values, the upper and middle branches meet to form an extinction point at $\tau_l = 139$ min. However, from Figure 1 in the work of Sharma et al. (1976), where a more complex consecutive reaction model was used and excellent agreement was shown for the simulation of the same experimental results, it seems that the upper and middle branches would persist to higher values of τ_l. Nevertheless, Figure 1 shows some capability of the model to describe real systems.

Throughout this work, all the physico-chemical parameters are as in Table 1 except when otherwise specified. These parameters are used simply because they represent a real system and also closely describe many other real systems.

An Adiabatic Case

Figure 3 presents the results of investigating the influence of the heat transfer coefficient, i.e., cooling effect, on the steady state multiplicity. It is shown that for an adiabatic case ($US = 0$), five steady states are possible for some values of τ_l while for a corresponding nonadiabatic case only three steady states exist. This is because in an adiabatic reactor, heat is much easier to build up and it is thus possible to ignite a higher temperature steady state. Thus, even a small heat loss by heat transfer

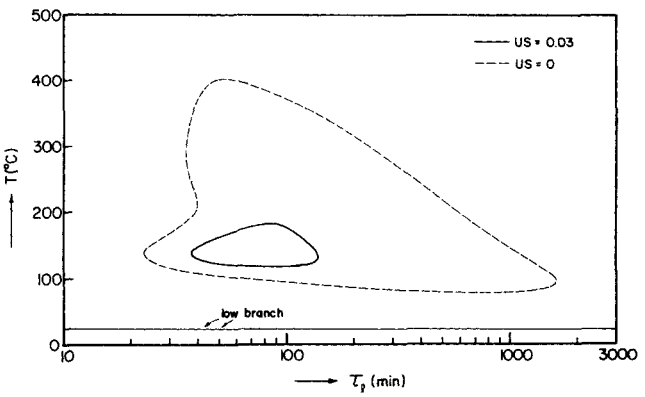

Figure 3. The influence of heat transfer coefficient on the steady state behavior.

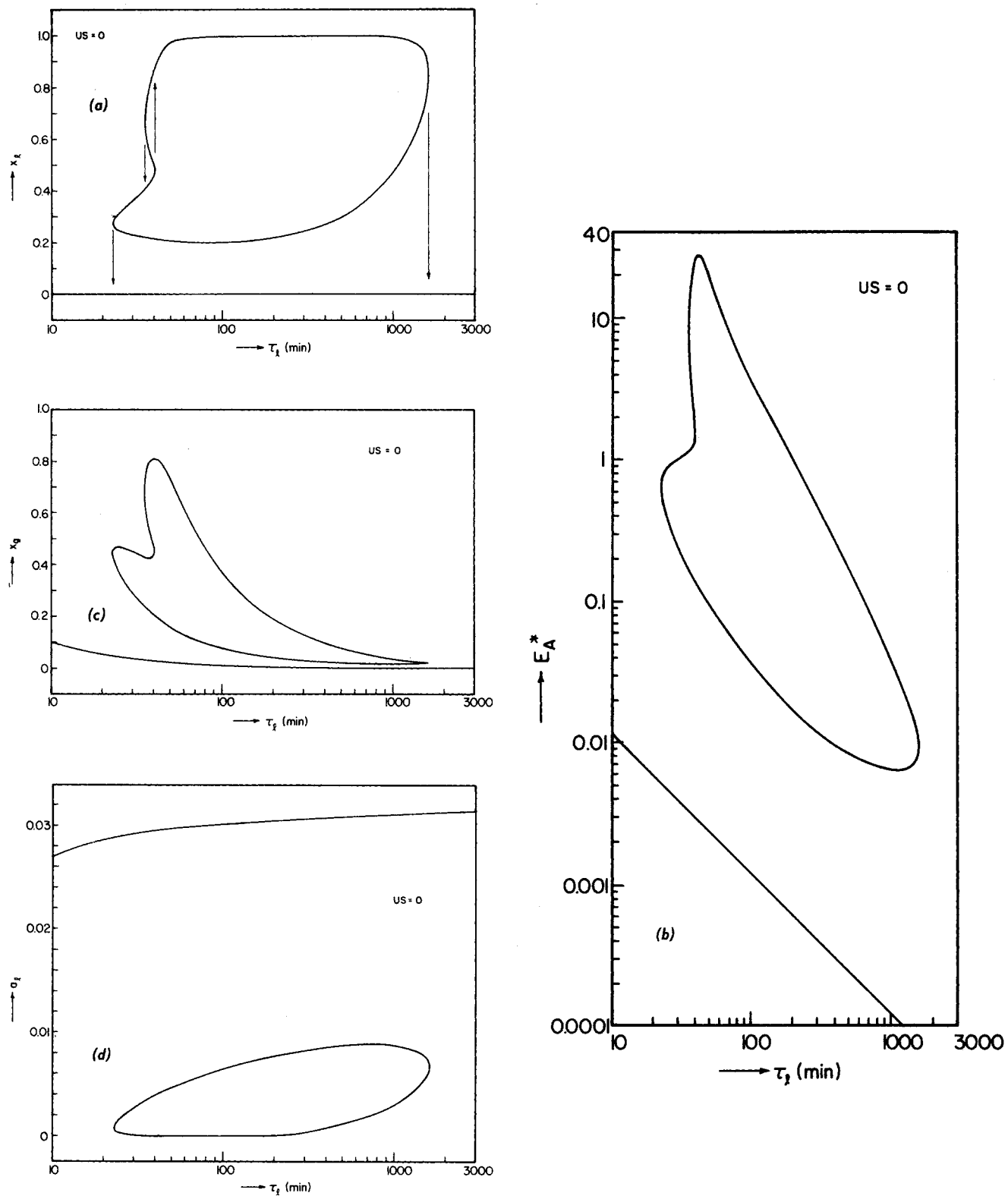

Figure 4. Effect of liquid residence time (an adiabatic case) on: (a) the conversion of liquid reactant; (b) the reaction factor; (c) the absorption of gaseous reactant; (d) the dimensionless liquid bulk concentration of gaseous reactant.

through the reactor wall or cooling device can have the dramatic effect of eliminating the possible existence of five steady states.

For the adiabatic case in Figure 3, the high temperature branch reaches a maximum and then comes down rapidly as the liquid residence time τ_l increases further, i.e., the liquid flow rate decreases and the ratio of the liquid to gas feed rates decreases. This is partly because the reaction rate decreases in that region as shown below, and at the same time, heat is continuously taken away by the flowing gas. However, the lower middle temperature branch, which should be unstable, comes down only slightly as τ_l increases over that range; this is related to having sufficient liquid reactant along that branch, as shown in Figure 4a. Thus, they finally meet each other and an extinction point is formed.

The possible existence of this type of isola with five steady states is an interesting feature of gas-liquid reactors which has

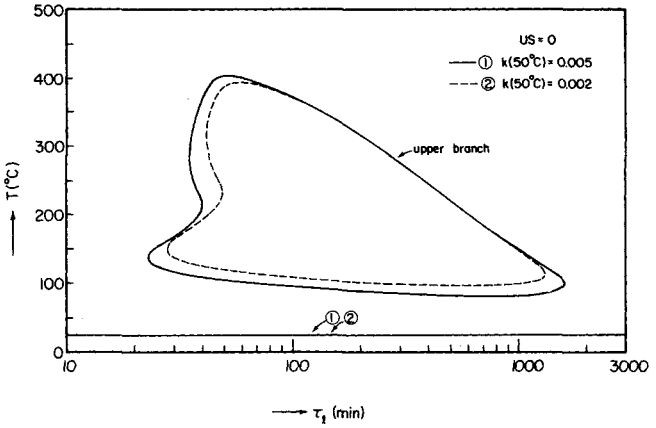

Figure 5. Effect of reactivity on the steady state temperature; an adiabatic case.

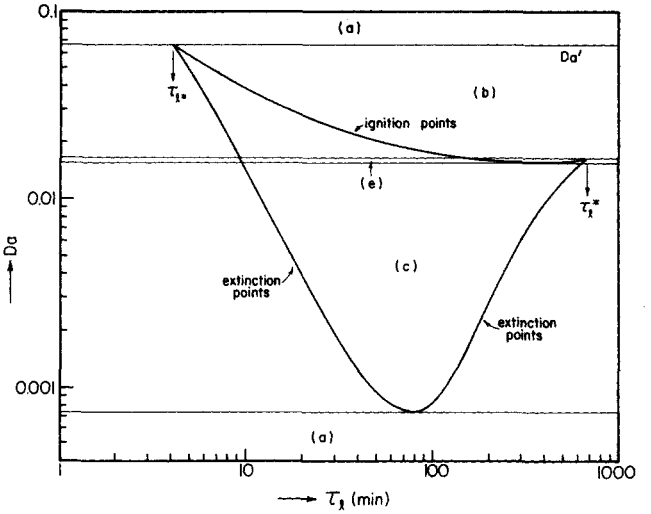

Figure 6. Effect of reactivity on the regions and patterns of steady state multiplicity.

not been observed before. The very existence of an isola in the adiabatic case is itself a special feature introduced by the two-phase nature, and is not present in single-phase CSTRs. It is suggested that the depletion of the liquid reactant plays an important role, as discussed below. We also note that the effect of the gas flow rate on the heat removal term of the energy balance Eq. 4 is important only for large values of τ_l, i.e., small values of F_l.

Figures 4a-d present the predictions of several related variables with respect to τ_l so that at a chosen τ_l their relationships can be clarified. Figure 4a shows that for certain values of τ_l, the upper branch corresponds to almost total conversion of the liquid reactant; thus, B_l is nearly zero over there. This, along with the related decrease of temperature as τ_l increases, causes the reaction factor to decrease sharply with increasing τ_l, as shown in Figure 4b, which means the reaction rate falls sharply. Note that the reaction factor is an indication of the rate of reaction. In turn, this causes the gas absorption rate to decrease and so does the total absorption of the gaseous reactant as shown in Figure 4c. However, from Figure 4d, it is seen that the dimensionless liquid bulk concentration of the gaseous reactant a_l generally increases as τ_l increases. This is mainly due to the sharp falling of the reaction rate so that the rate of consumption of the gaseous reactant in the "liquid film" decreases and more gaseous reactant goes into the liquid bulk even though the absorption rate actually decreases. Note that there are various interactions in gas-liquid reactors, which are rather complex but very interesting in that they lead to complicated behavior. Also note that five steady states are not observed in Figure 4d because those corresponding to the upper three temperature branches when five steady states exist have virtually zero a_l and so can not be distinguished.

Figure 5 shows the effect of reactivity on the steady state temperature. We note that the upper branch is quite insensitive to the variation of reactivity. This is because the limitation of the liquid reactant, instead of reactivity, dominates there. From Figures 2a and 2b, for the nonadiabatic case, the liquid reactant is not exhausted even on the upper branch and we see that the reaction factor varies quite smoothly. Thus, the upper branch leaves some room to show the effect of reactivity, as shown by comparing with the following figures. The steady-state temperature may be an important factor but it is the limitation of the liquid reactant which forces the reaction rate (thus temperature) to decrease sharply with increasing τ_l in the adiabatic case.

Uniqueness and Multiplicity Regions

In Figure 6, the effect of reactivity on the regions and patterns of multiplicity is shown by means of the critical values of τ_l. All the parameters are as in Table 1 except k (at 50°C) is varied to change the value of the Damköhler number, an indication of reactivity, defined as:

$$Da = \frac{aV_R H_o}{F_g} (k_o D_A B_{lf})^{1/2} \exp\left[\frac{2(-\Delta H_s) - E}{2RT_f}\right] \quad (25)$$

where the exponential term is added for convenience of presentation. Three multiplicity patterns are identified: (b) S-shaped, (c) isola, and (e) mushrooms. Region (a) means uniqueness for all values of the liquid residence time τ_l, while regions (b), (c) and (e) imply multiple steady states are possible for some values of τ_l. Note that for any value of $\tau_l < \tau_{l*}$ or $\tau_l > \tau_l^*$, as indicated in Figure 6, uniqueness is guaranteed for all values of Da. We also note that for Da values greater than Da', uniqueness is assured for all values of τ_l.

In Figure 6, it is also shown that as Da decreases, the range of τ_l values for which multiple steady states exist expands in both regions (b) and (e) but shrinks in region (c). In other words, as Da decreases, the left-hand-side ignition and extinction points go to higher values of τ_l while the right-hand-side points go to lower τ_l values. This is because as the reactivity decreases, the high temperature steady state can be ignited only at relatively larger liquid residence times (the left-hand ignition points), i.e., smaller liquid flow rates, for heat to build up or at smaller liquid residence times (the right-hand ignition points) to increase the ratio of the liquid to gas feed rates and thus the reaction rate. Similarly as Da increases, the high-temperature steady state tends to extinguish at higher values of τ_l (the left-hand extinction points) because of the heat loss through the liquid flow, or at lower τ_l values (the right-hand extinction points) because of the decrease of the ratio of the liquid to gas feed rates with increasing τ_l and the already lower reactivity. Note that the cause for the occurrence of the right-hand extinction point, which makes an isola in the adiabatic case, is in general the same for both the adiabatic and nonadiabatic cases, although for the nonadiabatic case the cooling effect is compounded.

Figures 7a-e show one of the mushrooms in region (e) with respect to different variables. Note that their behavioral features are quite similar to those of the corresponding Figures 3 and 4a-d of the adiabatic case, although only three steady states are possible here. It is clear that the same descriptions of their behavior and relationships for the adiabatic case can be applied here as well.

Figure 8 presents one example for the S-shaped multiplicity of region (b). The mushroom of Figure 7a is reproduced here with the dashed line. It is shown that although the reactivity varies so as to change the multiplicity pattern, the upper temperature branch is still insensitive to the reactivity, as shown also in Figure 5 for the adiabatic case. As compared to the case in Figures 2a and 3 (the nonadiabatic one), it may be suggested that as long as the liquid reactant is not fully exhausted, there is room

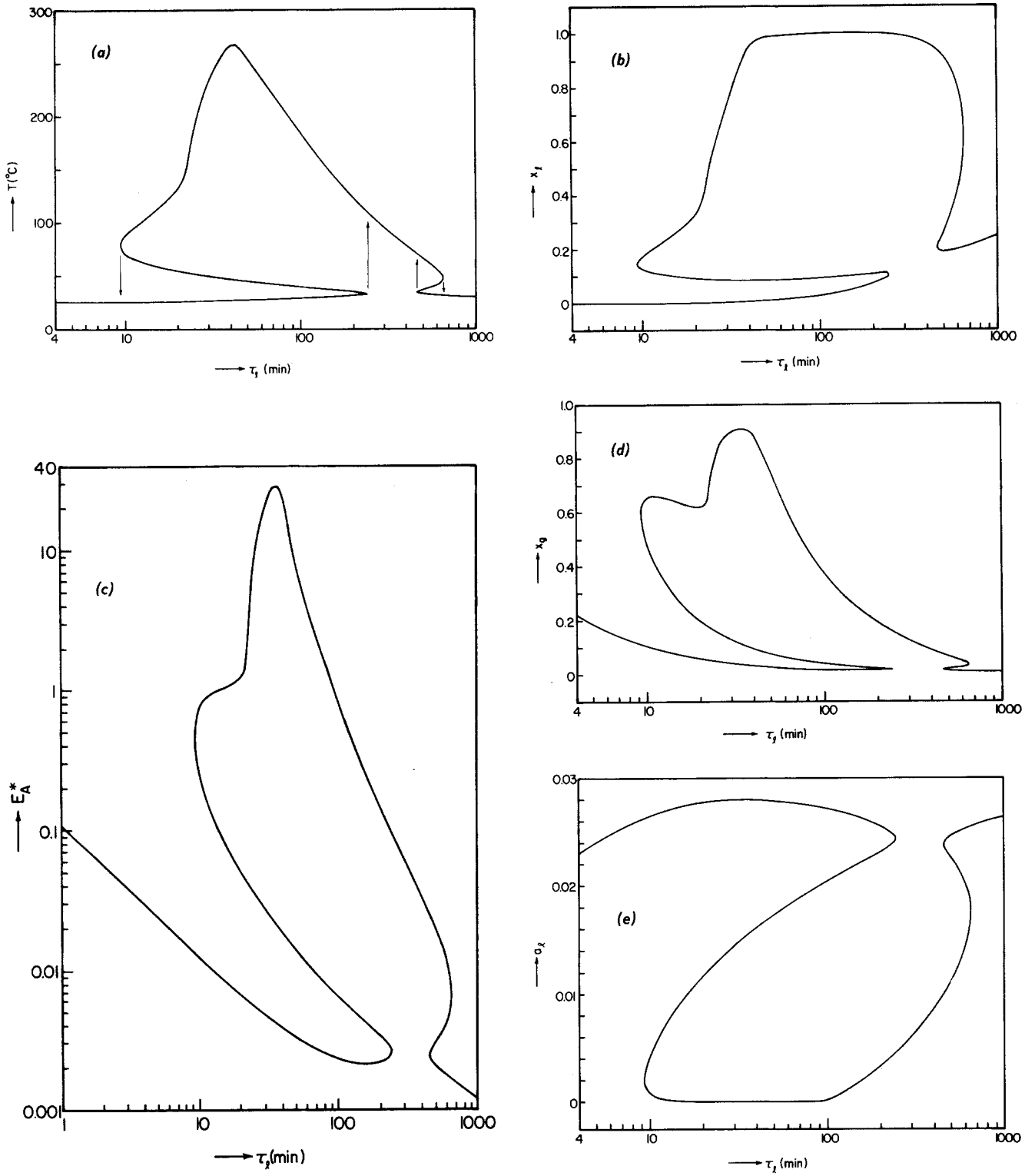

Figure 7. Effect of liquid residence time (k = 0.71, i.e., Da = 0.016) on: (a) the steady state temperature; (b) the conversion of liquid reactant; (c) the reaction factor; (d) the adsorption of gaseous reactant; (e) the dimensionless liquid bulk concentration of gaseous reactant.

for the upper temperature branch to vary with changing Da. In other words, as soon as the liquid reactant is completely consumed, the upper temperature branch will no longer be sensitive to changes in reactivity.

The effect of activation energy on the multiplicity regions is shown in Figure 9, where the region for E = 29 000 cal/gmol is the same as that in Figure 6 but with k (50°C) explicitly shown. It is clear that as the activation energy decreases, the multiplicity region shrinks with respect to both the reactivity and the liquid residence time.

As shown before (Figure 6), $\tau_l < \tau_{l*}$ assures a unique steady state with low temperature and low conversion of the liquid reactant for all values of Da. Noting that $F_{l2} \equiv V_l/\tau_{l*}$, Figure 10 presents a curve of these critical points as a function of the heat of reaction. Note that as the heat of reaction increases, the minimum liquid flow rate to guarantee uniqueness increases; this is because more heat needs to be removed from the reactor to avoid the formation of the high temperature steady state. Note that in Figure 10, a very small region of guaranteed

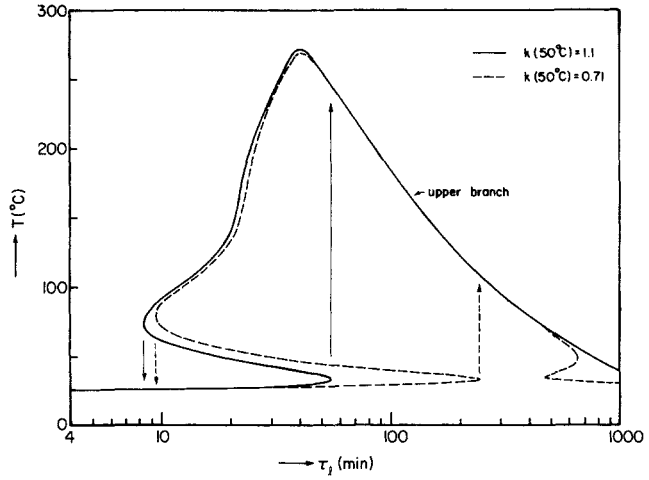

Figure 8. Effect of reactivity on the steady state temperature.

uniqueness exists under the multiplicity region (very close to the $F_l = 0$ Line) with the critical liquid flow rate corresponding to τ_l^*. However, that region is too small to be distinguished in Figure 10, and is therefore not shown.

CONCLUDING REMARKS

It is found that b_i is usually very close to unity, i.e., B_i is nearly equal to B_l, and the concentration profile of the liquid reactant is almost flat in the "liquid film." Note that the "liquid film" is theoretically proposed only to find the reaction factor E_A^* and the liquid bulk concentration of the gaseous reactant A_l, where E_A^* is used to describe the rate of gas absorption. A nearly unity b_i is observed because the ratio B_l/A_i is usually very high for any real system, and from very low to very high temperatures, noting that solubility decreases as temperature rises. Thus, the pseudo first order kinetics (i.e., $B_i = B_l$) can usually be applied to find E_A^* and A_l, and very accurate results can be obtained (for E_A^* and A_l only). Although not used in this work, the applicability of pseudo first order kinetics will mean considerable saving of numerical effort and computer time, and so should be quite useful in the design of gas-liquid reactors. Note that the previously mentioned pseudo-first-order *reaction* model assumes $B_l = B_{lf}$ and has nothing to do with the pseudo first order *kinetics* described above.

It is evident that assuming a nonvolatile liquid phase affects the adiabatic case much more than the nonadiabatic case, because the temperature is higher in the former. Since evaporation is not considered, the temperature on some portion of the high conversion branches may exceed the boiling point of the liquid phase. However, since our main interest is in the multiplicity *region*, and the ignition and extinction point temperatures are well below the boiling point, it is justifiable that the multiplicity *region* will not be affected to any significant extent by inclusion of evaporation. This is not, of course, true for actual temperature on the high conversion branches. One way to account for heat loss by evaporation of the liquid phase is to estimate the corresponding heat transfer coefficient, but some inaccuracy will result in the material balance of the model, which we found has only a small effect on the multiplicity *region*.

Finally, the possible existence of an isola with five steady states in an adiabatic reactor is an interesting prediction of the model. However, it is shown that even a small heat loss by heat transfer through the reactor wall or cooling device can eliminate the possibility of the existence of five steady states.

ACKNOWLEDGMENT

The Union Oil Fellowship in Reaction Engineering and a Reilly tuition scholarship for D. T.-J. Huang is gratefully acknowledged.

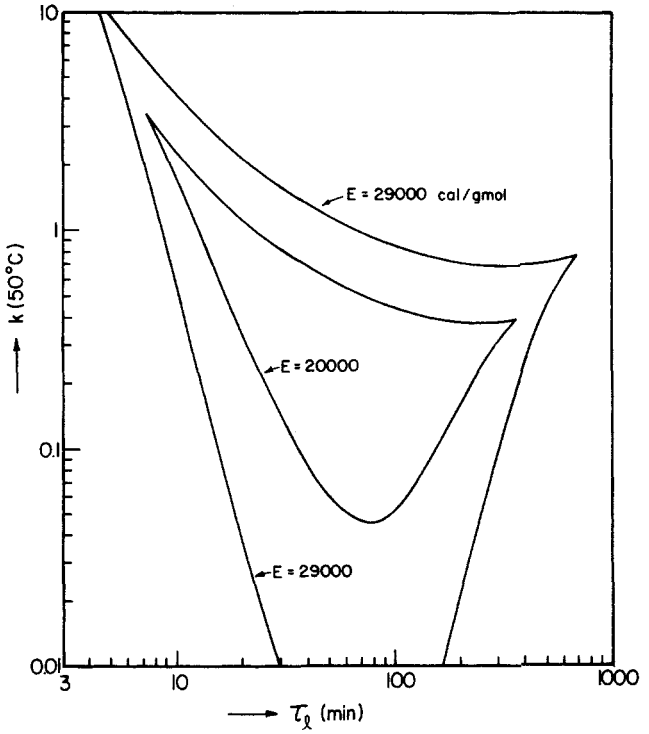

Figure 9. Effect of activation energy on the multiplicity regions.

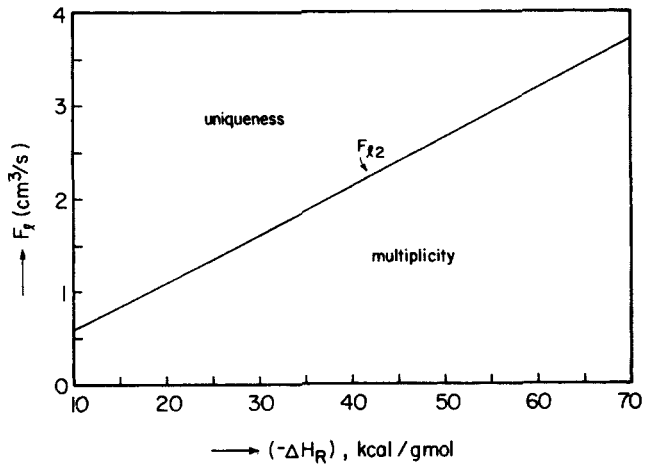

Figure 10. Effect of the heat of reaction on the critical liquid flow rates.

NOTATION

Those not listed here are defined by Eq. 13 in the text.

A	= concentration of gaseous reactant, gmol/cm³
a	= interfacial area per unit reactor volume, 1/cm
B	= concentration of liquid reactant, gmol/cm³
b_i	= dimensionless concentration, B_i/B_l
C_P	= molar heat capacity, cal/gmol · °K
D_A, D_B	= diffusion coefficients of species A and B respectively
Da	= Damköhler number, defined by Eq. 25
E	= activation energy, cal/gmol
E_A^*	= reaction factor
E_i	= instantaneous enhancement factor, defined by Eq. 9
F	= volumetric flow rate, cm³/s
H_o	= Henry's law constant
ΔH_R	= heat of reaction, negative if heat is liberated with reaction, cal/gmol
ΔH_s	= heat of solution, negative if heat is liberated with dissolution, cal/gmol
k	= second-order rate constant, cm³/gmol · s

k_o = second-order Arrhenius frequency factor, cm³/gmol · s
k_l = liquid mass transfer coefficient, cm/s
M = Thiele modulus or Hatta number, defined by Eq. 10
R = universal gas constant, cal/gmol · °K
R_A = reaction rate, gmol/cm³ · s
S = reactor cooling area, cm²
T = temperature, °K
U = overall heat transfer coefficient, cal/°K cm² · s
V_l = volume of liquid phase, $\epsilon_l V_R$, cm³
V_R = reactor volume, cm³
x_l = conversion of liquid reactant, $(B_{lf} - B_l)/B_{lf}$
y_{lb}, y_{ub} = dimensionless temperature bounds, defined by Eq. 23

Greek Letters

α' = dimensionless parameter, defined by Eq. 11
θ' = dimensionless parameter, defined by Eq. 11
ρ = molar density, gmol/cm³
ϵ_l = fractional liquid holdup in the reactor
τ_l = liquid residence time, V_l/F_l, s

Subscripts

c = cooling medium
f = feed
g = gas phase
i = gas-liquid interface
l = liquid phase

LITERATURE CITED

Ding, J. S. Y., S. Sharma, and D. Luss, "Steady State Multiplicity and Control of the Chlorination of Liquid n-Decane in an Adiabatic Continuously Stirred Tank Reactor," *Ind. Eng. Chem. Fundam.*, **13**, 76 (1974).

Hoffman, L. A., S. Sharma, and D. Luss, "Steady State Multiplicity of Adiabatic Gas-Liquid Reactors: I. The Single Reaction Case," *AIChE J.*, **21**, 318 (1975).

Huang, D. T.-J., and A. Varma, "Steady State and Dynamic Behavior of Fast Gas-Liquid Reactions in Non-Adiabatic CSTRs," *Chem. Eng. J.*, **21**, 47 (1981).

Raghuram, S., and Y. T. Shah, "Criteria for Unique and Multiple Steady States for a Gas-Liquid Reaction in an Adiabatic CSTR," *ibid.*, **13**, 81 (1977).

Sharma, S., L. A. Hoffman, and D. Luss, "Steady State Multiplicity of Adiabatic Gas-Liquid Reactors: II. The Two Consecutive Reactions Case," *AIChE J.*, **22**, 324 (1976).

Manuscript received May 2, 1980; revision received August 25, and accepted October 15, 1980.

II: Discrimination among Rival Reaction Models

The discrimination of the fast second-order, pseudo-first-order and fast pseudo-first-order reaction models on the basis of the second-order reaction model justifies the use of the pseudo-first-order model in the prediction of the multiplicity regions. The use of the fast second-order reaction model leads to a certain pitfall regarding uniqueness and multiplicity. Finally, the use of the fast pseudo-first-order reaction model is justifiable not only because of the fair agreement between the multiplicity regions predicted by this model and the second-order model but also because of the analyticity of the uniqueness and multiplicity regions obtained by this model.

SCOPE

In the operation of gas-liquid CSTRs (continuous stirred tank reactors), the occurrence of multiple steady states has been observed by Ding et al. (1974) for the chlorination of *n*-decane. Hoffman et al. (1975) and Sharma et al. (1976) have shown numerically the possible existence of five and seven steady states for single and consecutive second-order reactions respectively occurring in gas-liquid CSTRs. These have prompted development of *a priori* criteria providing conditions among physico-chemical parameters which assure unique and multiple steady states.

Raghuram and Shah (1977) derived analytic criteria, which they claimed to represent conditions assuring uniqueness of the steady state, and also presented various plots to determine the number of steady states in parameter space for the case of pseudo-first-order reactions (i.e., the conversion of the liquid reactant is assumed zero) and for the case of second-order reactions in the "fast" reaction regime, respectively. However, types of multiplicity patterns were not analyzed for either case.

We have recently (Huang and Varma 1981a) given *analytic* necessary and sufficient conditions for uniqueness, multiplicity and stability of the steady state, and also full view of the multiplicity regions and patterns under various operating conditions for the specific case of pseudo-first-order reactions in the "fast" reaction regime.

When multiple steady states exist, the steady state on the high temperature branch is generally in the "fast" reaction regime and the conversion of the liquid reactant is significant. On the other hand, the steady state on the low temperature branch is usually in the "slow" reaction regime. Therefore, applying any of the reaction models with the simplifying assumptions as mentioned above cannot cover the entire range of the multiplicity phenomenon and may lead to pitfalls. This raises the need to discriminate among various reaction models.

The main goal of this communication is to compare previously reported reaction models in a hope to justify some of the information obtained from these simplified models. The results of a fully second-order reaction model from Part I of this work (Huang and Varma, 1981b) are applied for this purpose. Types of multiplicity patterns for the cases of pseudo-first-order reactions and fast second-order reactions are also analyzed.

Correspondence concerning this paper should be addressed to A. Varma.

D. T.-J. Huang is presently at Brookhaven National Laboratory, Upton, New York 11973.